University of Nebraska - Lincoln
DigitalCommons@University of Nebraska - Lincoln

NASA Publications | National Aeronautics and Space Administration

1-1-1998

A new method of retrieving surface bidirectional reflectance from ground measurements: Atmospheric sensitivity study

A. I. Lyapustin
nNASA Goddard Space Flight Center

J. L. Privette
nNASA Goddard Space Flight Center

Follow this and additional works at: http://digitalcommons.unl.edu/nasapub

Part of the Physical Sciences and Mathematics Commons

Lyapustin, A. I. and Privette, J. L., "A new method of retrieving surface bidirectional reflectance from ground measurements: Atmospheric sensitivity study" (1998). *NASA Publications.* Paper 34.
http://digitalcommons.unl.edu/nasapub/34

This Article is brought to you for free and open access by the National Aeronautics and Space Administration at DigitalCommons@University of Nebraska - Lincoln. It has been accepted for inclusion in NASA Publications by an authorized administrator of DigitalCommons@University of Nebraska - Lincoln.

JOURNAL OF GEOPHYSICAL RESEARCH, VOL. 104, NO. D6, PAGES 6257–6268, MARCH 27, 1999

A new method of retrieving surface bidirectional reflectance from ground measurements: Atmospheric sensitivity study

A. I. Lyapustin
Universities Space Research Association, NASA Goddard Space Flight Center, Greenbelt, Maryland

J. L. Privette
NASA Goddard Space Flight Center, Greenbelt, Maryland

Abstract. Commonly, experimental data on surface directional reflectance are not properly corrected for atmospheric effects. In this paper, we describe a new method for rigorous retrieval of the bidirectional reflectance distribution function (BRDF) from ground-based measurements. It obtains the pointwise BRDF in the view directions and the best fit parameters of the approximating analytical model. Unlike previously developed algorithms, it can perform a retrieval using directional observations made at a single solar angle. This improvement allows one to process experiments with incomplete sets of measurements, such as those contaminated by clouds. The paper describes the performance of the method and its sensitivity to atmospheric parameters. Using rigorous direct modeling of the reflected radiance and developed inversion algorithm, we performed an analysis of BRDF errors, typical for measurements. It shows that the BRDF shape distortions due to diffuse irradiance are considerable in the visible and near-IR, even for low aerosol content in the atmosphere. This result confirms that an accurate atmospheric correction should be a required processing step in the experimental research of anisotropic surface reflectance.

1. Introduction

Experimental study of the directional reflective properties of vegetated land covers in the visible and near-IR parts of the spectrum was initiated by *Kriebel* [1974] in the early 1970s. *Lee and Kaufman* [1986] conducted one of the first theoretical simulations showing the significance of anisotropic effects in the remote sensing of vegetation from space. Now this is a rapidly evolving area of research encompassing different theoretical modeling and experimental branches. Interest in the BRDF of land covers is motivated by many reasons, including the potential indirect determination of plant parameters [*Privette et al.*, 1994], atmospheric correction of satellite images [*Vermote et al.*, 1997], land cover classification [*Strahler et al.*, 1996], and others.

A major problem in deriving the BRDF from measurements is accounting for diffuse skylight. *Deering and Eck* [1987] proved experimentally that the surface reflected radiance strongly depends on turbidity of the atmosphere. *Kriebel* [1974] and *Martonchik* [1994] developed accurate biconical reflectance/BRDF retrieval algorithms based on radiative transfer solutions. Both methods require measurements to be performed for a representative number of solar zenith angles and use interpolation techniques to obtain data at missing zenith and azimuthal angles.

This paper is not subject to U.S. copyright. Published in 1999 by the American Geophysical Union

Paper number 1998JD200123.

However, most publications report uncorrected surface reflectance. In this work, we show that accurate atmospheric correction is necessary in ground-based BRDF/albedo studies in the visible and near-IR spectral regions. This conclusion follows from rigorous simulations of the radiative fields over anisotropic surfaces and accurate inversions for the BRDF. The radiative transfer problem was solved with the spherical harmonics method [*Lyapustin and Muldashev,* 1998]. It takes into account all orders of scattering in the atmosphere and treats the boundary conditions analytically, which results in a high accuracy (on average, 0.2-0.3%) and speed of calculations. To process measurements, we developed an original BRDF retrieval algorithm based on principles of rotational symmetry and reciprocity. This paper describes the algorithm (section 2) and provides a systematic study of atmospheric effects in BRDF/albedo retrieval (sections 3 and 4). Section 5 analyzes the errors in typical BRDF measurements, induced by diffuse skylight. Experimental applications of our method will be given in future papers.

2. Algorithm

The lower boundary condition of the radiative transfer equation allows one to find the reflected radiance $I(\tau_0,\nu)$ in the direction ν for the specified surface BRDF $r(\nu',\nu)$

$$I(\tau_0,\nu) = S_\lambda \mu_0 r(\nu_0,\nu)\, e^{-\tau_0/\mu_0} + \frac{1}{\pi}\int_0^{2\pi} d\varphi' \int_0^1 r(\nu',\nu) I(\tau_0,\nu')\mu' d\mu' \tag{1}$$

Here S_λ is the extraterrestrial solar irradiance; τ_0 is the atmospheric optical thickness. The incidence and reflectance directions ν',ν are defined by zenith and azimuthal angles

(θ, φ), $\mu=\cos\theta$ and $\mu_0=\cos\theta_0$. In our notations, $\mu<0$ for the upward and $\mu'>0$ for the downward directions.

Let us assume that both the reflected and incident radiance fields are measured on some grid of angles with a sensor of small aperture that will let us deal with the bidirectional rather than with the biconical reflectance. Equation (1) provides the basis for determining the pointwise function $r(v_l', v_k)$. If the measurements of the sky and reflected radiance are performed for a complete set of solar zenith angles $\{\mu_0\}$, which includes all zenith view angles $\{\mu_{0n}\}\subset\{\mu_n'\}$, the discussed problem becomes the well known Fredholm equation of the 2nd kind with a known kernel $I(\tau_0, v')$. Under clear-sky conditions, it has a unique solution, which can be found with the resolvent method [*Mikhlin*, 1957].

At large optical thickness, the first term of (1) becomes negligibly small, and (1) turns into a Fredholm equation of the 1st kind. The inverse problem in this case is ill posed and requires a regularization in order to confine the multitude of plausible solutions.

We will consider only the experimentally significant case of medium to high transparency of the atmosphere. Owing to experimental constraints in field conditions or atmospheric instability, reliable measurements are frequently available only for a single or a small number of solar zenith angles. In this case there are insufficient data to use the standard way of solving the Fredholm equation. However, we can use a priori information on the general BRDF shape in a form of analytical model, whose parameters can be found from measurements made at single solar angle. The analytical model is required to extend the estimate of BRDF at a given solar angle θ_0 to the upper hemisphere of directions in order to evaluate the integral term of equation (1). The resulting BRDF in our algorithm is a composite function having accurate values in the directions of measurements, corresponding to measured intensities, and model values at other directions.

We require the analytical model to have properties of rotational symmetry and reciprocity. The first property implies that the BRDF depends only on relative azimuth. As mentioned by *Kriebel et al.* [1996], it holds as long as the surface has no strong linear structure. The principle of reciprocity follows from theoretical considerations [e.g., *DeHoop*, 1960]. They prove that the BRDF of structural surfaces is reciprocal as long as reflection from the surface primary element is reciprocal, which is generally true [*Snyder*, 1998]. Although *Kriebel* [1996] raised the question of the validity of reciprocity in experiments, he has only shown that the possible deviations are small.

The main mechanism behind the reciprocity violation is lateral inhomogeneity of the observed and surrounding area. First, it causes a nonzero horizontal photon transport from brighter to darker area, which breaks the reciprocity [*Girolamo et al.*, 1998]. Second, the averaging area, and therefore the degree of nonuniformity of the observed scene, depends on the view zenith angle. This may violate both reciprocity and rotational symmetry. Therefore we assume further that the BRDF measurements are performed in the far field and the field of view is large enough [*Snyder*, 1998]. Practically, this means that the observed area at all view angles should be much larger than the size of primary structure elements of the surface.

Let $I(v_0, v_i)$ and $I_i^{(n)}(v_0, v_i)$ denote the measured radiance in the direction v_i and the theoretical radiance at nth iteration, respectively. To solve the problem, we use the following iterative algorithm: (1) Calculate

$$r_i^{(n)} = r_i^{(n-1)} + \alpha\,\Delta r_i^{(n)}, \tag{2}$$

where

$$\Delta r_i^{(n)} = e^{\tau_0/\mu_0}\{I(v_0, v_i) - I_i^{(n-1)}(v_0, v_i)\}/S_\lambda\mu_0, \tag{3}$$

and α is a relaxation parameter (weight factor) which accelerates convergence. (2) Find the best fit parameters of the analytical BRDF model for the pointwise function $r_i^{(n)}$. (3) Compute the theoretical radiance $I_i^{(n)}(v_0, v_i)$ for the composite BRDF, which is equal to $r_i^{(n)}$ at angles v_i and to the values of analytical model at other directions. (4) Evaluate the standard deviation $\sigma\{I(v_0, v_i) - I_i^{(n)}(v_0, v_i)\}$. (5) Repeat steps 1-4 until $\sigma\le\varepsilon$, where ε is a given error threshold.

The use of the composite function allows us to retain specific features of measured reflectance in the directions of measurements, which may be useful in the validation of BRDF models and retrieval of surface physical properties. Parameters of the analytical BRDF model potentially have a number of applications, from realistic radiative transfer simulations to land cover classification. Note that the choice of the analytical model has no significant effect on the retrieval as long as the model fits well the general shape of the measured BRDF.

As an analytical BRDF model, we employ the Rahman-Pinty-Verstraete (RPV) function [*Rahman et al.*, 1993] depending on 3 parameters (ρ, k, g). This empirical model is flexible enough to approximate the surface reflectance well [*Engelsen et al.*, 1996] and has the highest accuracy among 10 commonly used models in predicting nadir reflectance and surface albedo [*Privette et al.*, 1997].

To solve the best fit problem in step 2, we use the modified RPV (MRPV) function, where the Heney-Greenstein term is substituted by an exponential function $\exp(b\cos\gamma)$, where γ is a scattering angle. This modification of *Martonchik et al.* [1998] allows one to linearize the MRPV function for an efficient inversion. We use the following algorithm: logarithmic transformation of the MRPV function R linearizes it for the unknowns k and b

$$\ln R = (k-1)\ln\mu\mu_0(\mu+\mu_0) + b\ln\cos\gamma + \ln\rho\left(1+\frac{1-\rho}{1+G}\right) \tag{4}$$

Parameters k, b, ρ are then found from the least squares problem,

$$F = \sum r_i^2(\ln R_i - \ln r_i)^2 = min\{k, b, \rho\} \tag{5}$$

which is expanded into three explicit equations following from

$$\partial F/\partial k = 0,\ \partial F/\partial b = 0,\ \partial F/\partial\rho = 0 \tag{6}$$

The first two equations, linear in parameters k and b, can be solved with respect to these two parameters. The corresponding expressions are substituted into the third equation, which gives the nonlinear equation for the unknown ρ, $f(\rho)=0$. The function $f(\rho)$ is continuous and takes opposite signs on the borders of interval $[0, \bar{\rho})$, which confines the range of parameter ρ. The value $\bar{\rho}$ is an arbitrary large

number, say, $\bar{\rho}$ =100. On the basis of these properties, we use the Wijngaarden-Dekker-Brent algorithm [*Press et al.*, 1992] to find a root of $f(\rho)$=0. Having found ρ, it is easy to find parameters k and b analytically. Compared to nonlinear minimization, this approach is much faster and less demanding of computational resources.

The form of the merit function, $F = \sum r_i^2 (\ln R_i - \ln r_i)^2$, provides an unbiased solution equivalent to the result of minimization of the standard form $F_{st} = \sum (R_i - r_i)^2$. To prove that, it is sufficient to show that $F \to F_{st}$ in the vicinity of the minimum. Near the minimum, $R_i/r_i = 1 + \delta_i$, where $\delta_i << 1$ for all i, provided that the analytical function R_i approximates the measurements uniformly. Therefore one can expand the logarithm into a Taylor series retaining only a linear term,

$$r_i(\ln R_i - \ln r_i) = r_i \ln {R_i}/{r_i} \to r_i \delta_i = R_i - r_i \qquad (7)$$

which leads us to the standard form F_{st}.

Another form of merit function, $\sum (\ln R_i - \ln r_i)^2$, is sensitive to noise in the data, which may bias the solution. In this case, the random errors of measurements ε_i are amplified in the vicinity of the minimum as ε_i/r_i since $r_i<1$ or even $r_i<<1$ in the meaningful domain of view angles, except for relatively large ones where $r_i \geq 1$.

On the basis of the described iterative scheme, we have developed two algorithms. The first one inverts (1) for the function $r(\mu', \mu, \varphi - \varphi')$ based on measurements of the incident and reflected radiance. In this case, the integral term of (1) is estimated using trapezoidal quadrature. The second algorithm involves the radiative transfer calculations to compute the radiance $I_i^{(n)}(v_0, v_i)$ in step 3. This algorithm does not require the measurements of skylight but relies on ancillary information about the atmospheric optical properties. In the next two sections, we discuss the performance of these algorithms and describe their sensitivity to the atmospheric and geometrical conditions.

3. Properties of Numerical Scheme

First, we will establish some important properties common to both algorithms.

3.1. Range of Validity

At small and medium atmospheric opacity ($\tau \leq 0.7$), the algorithm's convergence is stable and fast. It is not sensitive to the initial estimate of BRDF, which becomes an issue at larger optical thickness. The initial estimate can be obtained either from the direct or from the total surface irradiance

$$r^{(0)}(v_0, v) = e^{\tau_0/\mu_0} I(v_0, v) / S_\lambda \mu_0 \qquad (8a)$$

$$r^{(0)}(v_0, v) = \pi I(v_0, v) / F(\mu_0) \qquad (8b)$$

where $F(\mu_0)$ is the total downward flux. To obtain the estimate (8a), one needs to know only the aerosol optical thickness. However, (8a) neglects the contribution of the diffuse incident radiance, which becomes increasingly important as the optical thickness and solar zenith angle increase. This effect can be seen from Figure 1 showing the corresponding decrease of the relative direct flux (F_{dir}/F). Since our algorithm requires the first term of equation (1) to be not negligible compared to the second term, the optical thickness should not exceed some critical value (τ^{max}) for the sake of convergence. The value τ^{max} obtained in numeric simulations for nonabsorbing aerosol is shown in Figure 2. Calculations show that the value $\tau^{max}(\theta_0)$ is virtually independent of the aerosol scattering function, or in other words, of the size distribution of aerosol particles. This value can be translated into the ratio of fluxes which gives the

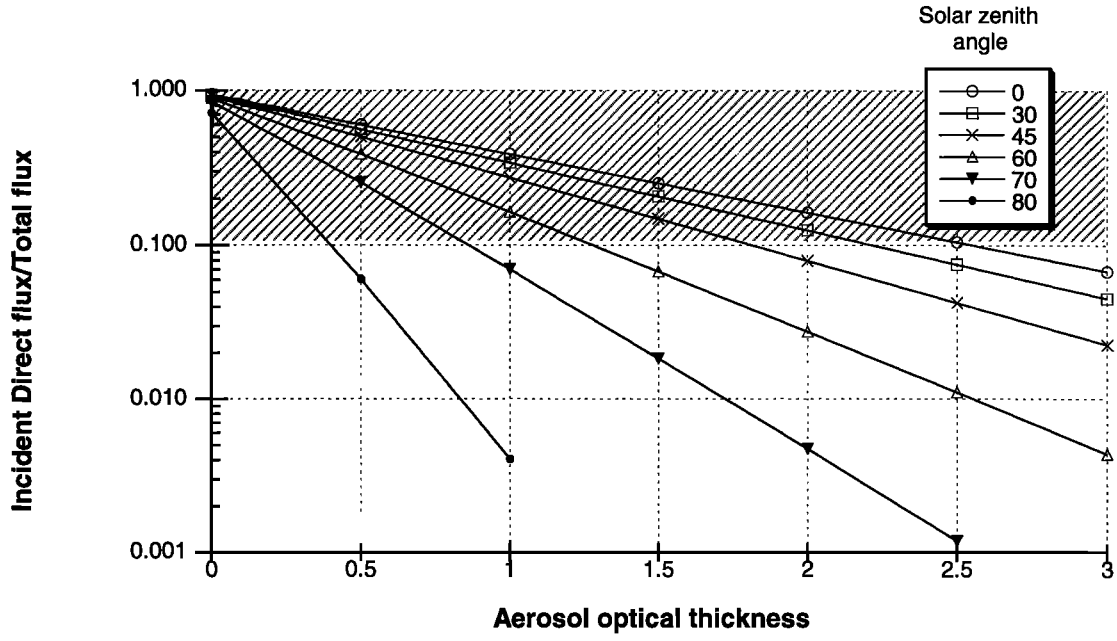

Figure 1. Ratio of the direct to the total incident flux (F_{dir}/F) as a function of the optical thickness and solar zenith angle (SZA) at 0.55 μm. The bidirectional reflectance distribution function (BRDF) retrieval algorithm is valid in the selected range of $F_{dir}/F \geq 0.1$-0.15.

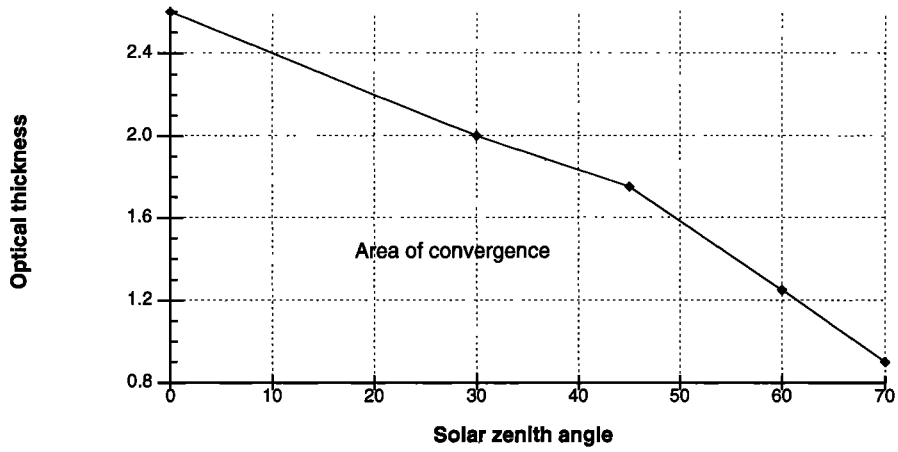

Figure 2. Range of atmospheric optical thickness where the initial approximation (8a) works.

constraint of validity $F_{dir}/F \geq 0.1$-0.15. From Figures 1 and 2 it follows that the range of possible atmospheric conditions is wide at high Sun but narrows sharply at low Sun ($\theta_0 > 70^\circ$). Obtaining an initial estimate with (8b) lifts the described limitations. For example, we achieved the convergence at $\tau=2.6$ and $\theta_0=65^\circ$. However, this way requires a more detailed knowledge of aerosol properties for the calculation of incident flux.

In most circumstances, atmospheric conditions fall within the range $\tau \leq 0.7$ (at $\theta_0 \leq 75^\circ$) and formula (8a) can be used. Notice that the described limitation on optical thickness follows from the properties of the adopted numerical scheme and has nothing to do with the fundamental transition of equation (1) from the Fredholm equation of the 2nd kind into equation of the 1st kind. This constraint comes into effect when the direct incident flux becomes commensurable with the noise level.

3.2. Number of Iterations to Convergence and Weight Factor

The weight factor α is assumed to be constant throughout the iterations. Depending on optical thickness, it can be selected optimally to maximize convergence. Figure 3 shows the optimal weight factor as a function of the atmospheric optical thickness and the corresponding minimal number of iterations for a medium solar angle of 45°. Iterations stopped at $\sigma < 0.5 \times 10^{-4}$, which means that the measured radiance was approximated at an accuracy of better than 0.1-0.3%. As one can see, at $\tau < 0.7$ and optimal weight, this algorithm is very efficient and requires only two to six iterations.

4. Sensitivity Study

The developed algorithms compute the contribution of the skylight into reflected radiance, or the integral term in (1), differently. The second algorithm, based on the radiative transfer solution, accurately calculates this term for an assumed aerosol model independently of the geometry of observation (the overall interval and the number of view angles). In contrast, the first algorithm does not depend on an aerosol assumption, but it is sensitive to the geometry of measurements. Below, we study the sensitivity of the first algorithm to the geometrical effects and the second algorithm to the atmospheric effects. The analysis was performed for two surface types, grass [*Myneni and Asrar*, 1993] and plowed field [*Kriebel*, 1974]. The grass is dark in the visible with an albedo $q(45^\circ) \approx 0.028$, and bright in the near-IR, with $q(45^\circ) \approx 0.42$. The plowed field has a medium reflectance with nearly constant albedo, 0.17 in the visible and 0.18 in the near-IR.

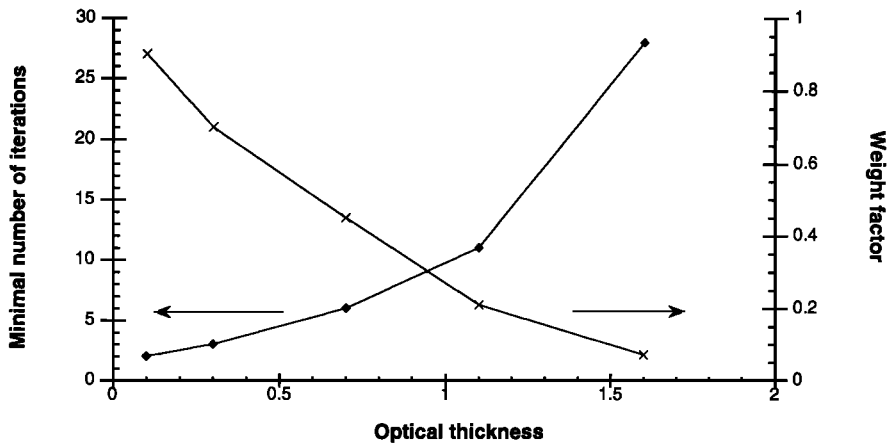

Figure 3. Optimal weight factor (crosses) as a function of the atmospheric optical thickness and the corresponding minimal number of iterations (diamonds) for a medium SZA 45°.

4.1. Atmospheric Effects

Initially, we have simulated the reflected radiance for the aerosol scattering function of *Elterman* [1968] at 0.75 μm (EL075) with asymmetry of scattering $<\cos\gamma>=0.58$ and absorption $\omega^a=0.95$. The atmosphere was modeled as a vertically uniform mixture of air molecules and aerosol particles with loading varying from $\tau^a=0.1$ (clear) to $\tau^a=1$ (hazy).

In the retrieval procedure, the aerosol optical thickness was modified by ±40% and ±20% for the clear and hazy cases, respectively, and aerosol absorption was varied in the range $\omega^a=0.8$-1. The asymmetry of scattering $<\cos\gamma>$ was varied from 0.48 (indicatrix of Elterman at 0.55 μm, EL055) to 0.72 (indicatrix of *Krekov and Rahimov*, [1982] at 0.6943 μm, KR069). These variations of the input aerosol parameters overlap the typical range for continental aerosols and marginally exceed possible errors of measurements.

The results of this study are presented in Table 1. The first row of the table gives the correct solution. The other rows present solutions obtained with the deviated parameter τ^a or ω^a or with the different scattering function. The error of solution is roughly a linear function of errors in the input aerosol parameters, which allows one to estimate the realistic expected accuracy of retrieval. Since the solution is represented by three parameters of the MRPV model, all of which shift as we perturb the input parameters, we also use surface albedo as an integral measure of sensitivity. Albedo itself changes with atmospheric optical thickness, so we restrict ourselves to simulations at solar zenith angle of 50°, when this effect is minimal [*Lyapustin*, 1999].

Results of Table 1 show that if the atmosphere is clear, reasonable variations in the aerosol model have little effect on the retrieved albedo (1-2% of magnitude). At $\tau^a\leq 0.5$, the error in the input parameters $\Delta\tau^a/\tau^a=20\%$ or $\Delta\omega^a=\pm 0.05$ or $\Delta<\cos\gamma>=\pm 0.12$ give the same error $\Delta q/q\leq \pm 3$-4%. Parameters ρ and especially b are subject to a factor of 2-3 larger variations. For a hazy atmosphere, uncertainty in aerosol absorption will most likely cause the largest error. At typical error $\Delta\omega^a\leq\pm 0.05$ [e.g., *Hobbs et al.*, 1997], the error in surface albedo does not exceed 10%. The same error may be caused by the variation of aerosol scattering function.

Table 1 also reveals an interesting selective sensitivity of retrieved MRPV parameters to the individual aerosol input parameters. Parameter ρ is primarily affected by the variation in aerosol absorption, and parameter b depends more on the aerosol optical thickness. Parameter k is mainly defined by the anisotropy of reflectance and is not very sensitive to the aerosol characteristics. Using the major influential factor only, one can write in a functional form $\rho\approx f_1(\omega^a)$ and $b\approx f_2(\tau^a)$. This selective sensitivity seems to be an interesting subject for future research.

Thus, at small and medium aerosol loading, the uncertainty in atmospheric parameters results in rather small error (≤3-4%) in the retrieved surface albedo. At the same time, individual parameters of the MRPV model have a noticeable

Table 1. Aerosol Effect on Retrieval of Bidirectional Reflectance Distribution Function (BRDF) and Albedo at Different Atmospheric Opacities (τ^a=0.1, 0.5, 1.0) at 0.65 μm

	Grass				Plowed field			
τ^a; ω^a	ρ	k-1	b	q	ρ	k-1	b	q
0.10; 0.95	0.0132	-0.1955	0.5737	0.0276	0.0612	-0.3378	0.9303	0.1728
0.14; 0.95	0.0132	-0.1967	0.5909	0.0282	0.0609	-0.3383	0.9568	0.1749
0.06; 0.95	0.0131	-0.1941	0.5574	0.0275	0.0613	-0.3374	0.9061	0.1708
EL055	0.0133	-0.1959	0.5771	0.0280	0.0612	-0.3386	0.9396	0.1739
KR069	0.0131	-0.1942	0.5696	0.0276	0.0611	-0.3357	0.9207	0.1715
0.10; 1.0	0.0131	-0.1955	0.5766	0.0276	0.0605	-0.3378	0.9358	0.1716
0.10; 0.8	0.0135	-0.1950	0.5656	0.0284	0.0631	-0.3382	0.9194	0.1768
0.50; 0.95	0.0130	-0.1977	0.5835	0.0277	0.0609	-0.3399	0.9313	0.1738
0.60; 0.95	0.0131	-0.2028	0.6272	0.0286	0.0601	-0.3459	1.0008	0.1793
0.40; 0.95	0.0129	-0.1920	0.5448	0.0268	0.0615	-0.3344	0.8661	0.1683
EL055	0.0132	-0.2011	0.6081	0.0286	0.0608	-0.3441	0.9743	0.1784
KR069	0.0127	-0.1926	0.5558	0.0266	0.0610	-0.3323	0.8784	0.1677
0.50; 1.0	0.0124	-0.1987	0.5985	0.0267	0.0576	-0.3409	0.9566	0.1669
0.50; 0.8	0.0149	-0.1933	0.5419	0.0310	0.0715	-0.3369	0.8649	0.1950
1.00; 0.95	0.0127	-0.2049	0.6130	0.0278	0.0607	-0.3412	0.9345	0.1740
1.20; 0.95	0.0128	-0.2202	0.7023	0.0296	0.0580	-0.3584	1.0915	0.1848
0.80; 0.95	0.0127	-0.1883	0.5185	0.0261	0.0621	-0.3261	0.8057	0.1636
EL055	0.0131	-0.2112	0.6570	0.0293	0.0597	-0.3509	1.0279	0.1824
KR069	0.0123	-0.1946	0.5470	0.0258	0.0609	-0.3290	0.8350	0.1634
1.00; 1.0	0.0114	-0.2086	0.6481	0.0255	0.0534	-0.3455	0.9945	0.1576
1.00; 0.8	0.0171	-0.1920	0.5128	0.0351	0.0844	-0.3303	0.8010	0.2206

The first row of each section gives the accurate aerosol and BRDF model parameters. Other data represent solutions with the aerosol optical thickness, scattering function, and absorption assumed with errors.

sensitivity to the aerosol model. Presently, parameters of the purely mathematical MRPV model are not related to the physical properties of surface, which could drive the accuracy requirements. Unless this relation is established, we hesitate to specify the secondary accuracy requirements for the ancillary aerosol data since surface albedo is not very sensitive to the aerosol model. Alternatively, such requirements may be established, for example, in the problem of land cover classification based on separability of classes in the phase space that includes three MRPV/RPV parameters. This, however, is also a subject of future research.

We used the RPV model in forward calculations and the MRPV model in the inversion. Both functions originate from the model of *Minnaert* [1941] and have approximately the same capabilities in fitting the experimental BRDF. In the error budget, however, one may anticipate the largest errors in case when the MRPV model poorly fits the general shape of the real BRDF. To avoid this situation, we plan to use a representative set of parametrical BRDF models, for example, those valid in different radiative transfer regimes in plant canopies [*Privette et al.*, 1997] and select the optimal one using the best fit criteria.

4.2. Geometry of Measurements

The accuracy of the first algorithm is limited by the accuracy of evaluation of the integral term of (1), which in

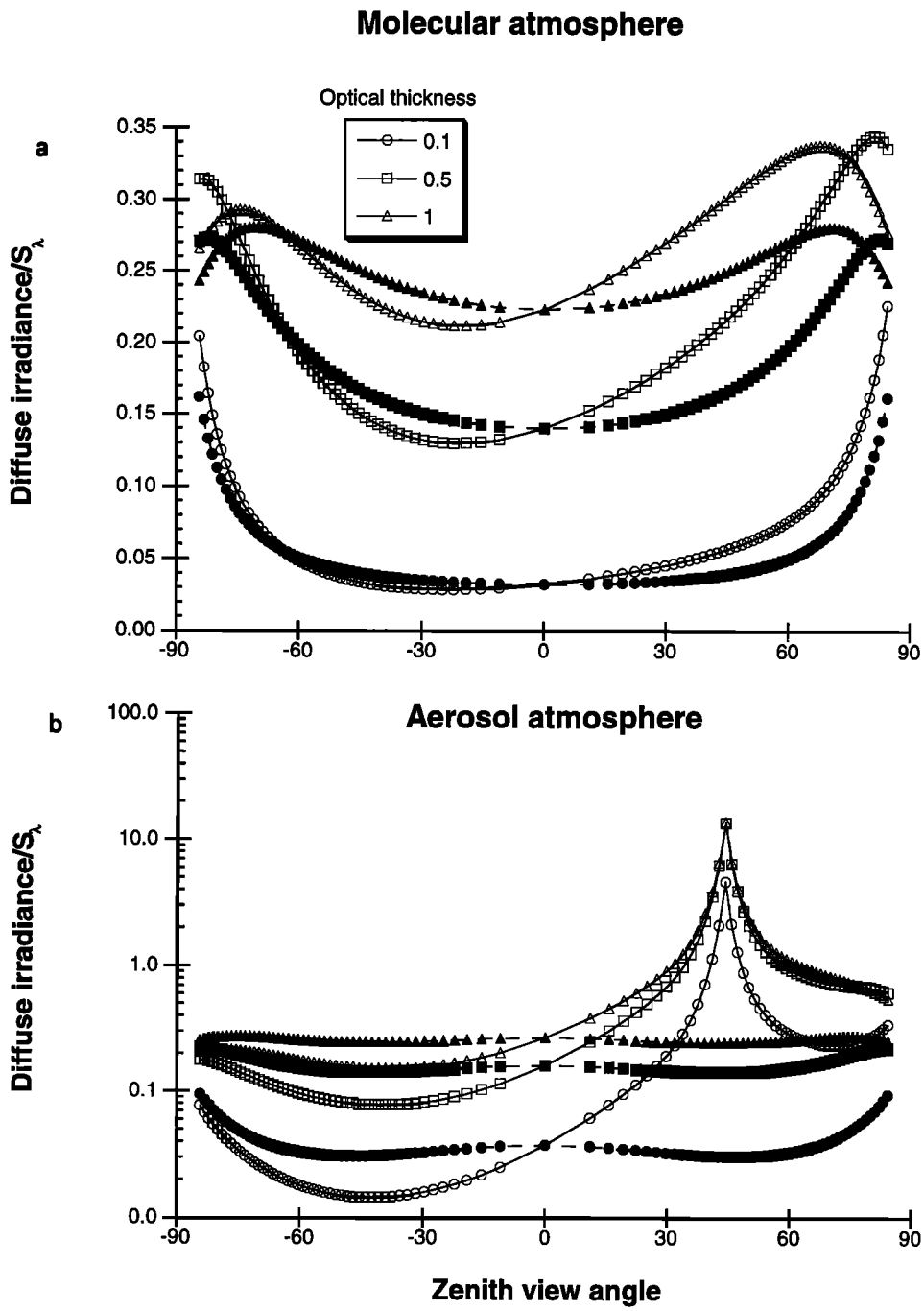

Figure 4. Angular dependence of the normalized downward diffuse radiance for different optical thickness of the atmosphere, showing the radiance in (a) molecular and (b) aerosol (scattering function EL075) atmospheres. The open and solid symbols correspond to the principal and cross planes, respectively.

turn depends on the geometry of measurements. Typically, the incident and reflected radiance are measured on an equidistant angular grid with 10-15° zenith and 30-45° azimuthal grid steps [*Kriebel*, 1974; *Deering and Leone*, 1986]. The range of zenith angles is usually restricted to $10\text{-}15^\circ \le \theta \le 75^\circ$. This limitation leads to some underestimation of the integral term in (1). As a result, the minimal residual error σ in this algorithm, as our calculations show, does not decrease below 10^{-3}-10^{-4}.

Since the grid of angles is rather sparse, the anisotropy of the sky radiance can be an additional source of errors. Over land, the scattering function is usually characterized by a strong forward scattering peak, so the diffuse radiance in the Sun aureole may exceed the average sky radiance by orders of magnitude. For example, Figure 4 shows the incident radiance for the aerosol-free (a) and purely aerosol (b) atmosphere with aerosol scattering function EL075. The aureole area, as one can see, may extend up to 10°. If one of the sky radiance measurements falls into the sun aureole area, the integral term will be considerably overestimated and the resulting BRDF underestimated.

We investigated the effect of the number of zenith view angles N_a in the range $0 \le \theta \le 75^\circ$ at $\Delta\varphi = 30^\circ$ on the accuracy of BRDF/albedo retrieval. Table 2 shows the corresponding dependence of the surface albedo on N_a for the plowed field. The results presented in the second row of the second and third columns illustrate the case when one of the view angles is very close to the direction of sun causing considerable underestimation of albedo. In the last column, the solar angle was shifted to avoid this situation.

The cases N_a =6, 8 correspond approximately to the 15° and 10° zenith angle grid steps. All other conditions being equal, the accuracy of the solution at grid step 10° will be higher. Though it is not straightforward given the overall small number of view angles, the increase of N_a in general allows one to obtain a higher signal-to-noise ratio and to better characterize the BRDF.

5. Accuracy of BRDF Measurements

Most experimental BRDF reports fall into three major groups: (1) an apparent reflectance, $R_1 = I/S_\lambda \mu_0$, [*Eaton and Dirmhirn*, 1979; *Deering and Eck*, 1987]; (2) BRDF given by (8a), partially corrected for the direct illumination, R_2, and (3) reflectance, obtained with a reference panel R_3 (8b), [e.g., *Kimes et al.*, 1986; *Kimes and Newcomb*, 1987]. Measurements of the third group are most accurate, however none of these groups gives the true BRDF. Thus, a significant amount of data in the currently accumulated databases of the spectral-directional surface reflectance have only approximate or no correction for atmospheric effects. Moreover, until now the magnitude of atmospheric distortions in the reported BRDF has not been clear.

Table 2. Dependence of Retrieved Surface Albedo on Number of Zenith View Angles in the Range $0 \le \theta \le 75^\circ$.

N_a	$q(45^\circ)$, τ^a=0.1	$q(45^\circ)$, τ^a=0.4	$q(35^\circ)$, τ^a=0.4
6	0.1608	0.1327	0.1770
8	0.1722	0.1706	0.1732
10	0.1741	0.1763	0.1701
12	0.1736	0.1739	0.1674
True albedo	0.1697	0.1709	0.1689

Azimuth grid size is 30°. The last row gives the accurate albedo at 0.75 μm given the solar angle and aerosol optical thickness.

To fill this gap, we present the results of an error study for the reflectance factors R_1-R_3 at three wavelengths, 0.45, 0.65 and 0.85 μm. Figures 5a and 5b show the relative errors (r/R-1, %) in the principal plane for grass in the visible and near-IR ranges. One can see that the BRDF is always underestimated in group 1 and overestimated in group 2. Group 2 gives the largest error proportional to the relative diffuse incident flux. Group 3 gives the "centered" reflectance factor, so that after being integrated over angles, it should predict the albedo, which is accurate to the factor of multiple reflections between the surface and the atmosphere. However, even in this group at τ^a=0.1 the shape of BRDF can be considerably distorted, up to ±12% in the red and ±8% in the near-IR.

Figures 6a and 6b show the relative errors in the corresponding MRPV parameters and surface albedo in groups 2 and 3. The errors are considerable in group 2 when albedo for the aerosol-free atmosphere is overestimated by up to 19% at 0.45 μm, by 5% at 0.65 μm, and by 2.4% at 0.85μm. At τ^a=0.1, these errors increase up to 39%, 18%, and 19%, respectively. In group 3, deviation of albedo from the accurate value is due to the multiple reflection of light between the surface and the atmosphere. The effect is stronger over a brighter surface.

Over surfaces of medium and high reflectance, the errors shown may considerably exceed the tolerance of climatologic models that require an accuracy of ±0.02 in the global albedo data sets [*Sellers*, 1993]. A review by *Henderson-Sellers and Wilson* [1983] shows that different climate models predict a significant response of the global climate temperature to the uncertainty $\Delta q = \pm 0.01$, from ∓ 0.2 to ∓ 2 K. This means, in turn, that more accurate climate modeling will require a more stringent knowledge of the global surface albedo, which is unattainable without proper atmospheric correction.

6. Conclusions

We have described a new algorithm for the accurate retrieval of surface BRDF from ground-based measurements. Compared to methods of *Kriebel* [1974] or *Martonchik* [1994], which need measurements at a representative number of solar zenith angles, our method is able to obtain the BRDF from measurements at a single solar angle. This improvement allows one to process field data despite an incomplete set of measurements, as may be the case on partly cloudy days. On the other hand, our method works similarly to the method of Martonchik if measurements are available for many solar angles. The main difference in this case is the method of BRDF interpolation; instead of spline interpolation, we use a parametric BRDF model.

The accuracy of BRDF/albedo retrieval is limited by our approximate knowledge of aerosol parameters. At maximal uncertainty, the error in surface albedo determined by the retrieved BRDF does not exceed ±3-4% at $\tau^a \le 0.5$. The errors of MRPV parameters ρ and b can be a factor of 2-3 higher. At

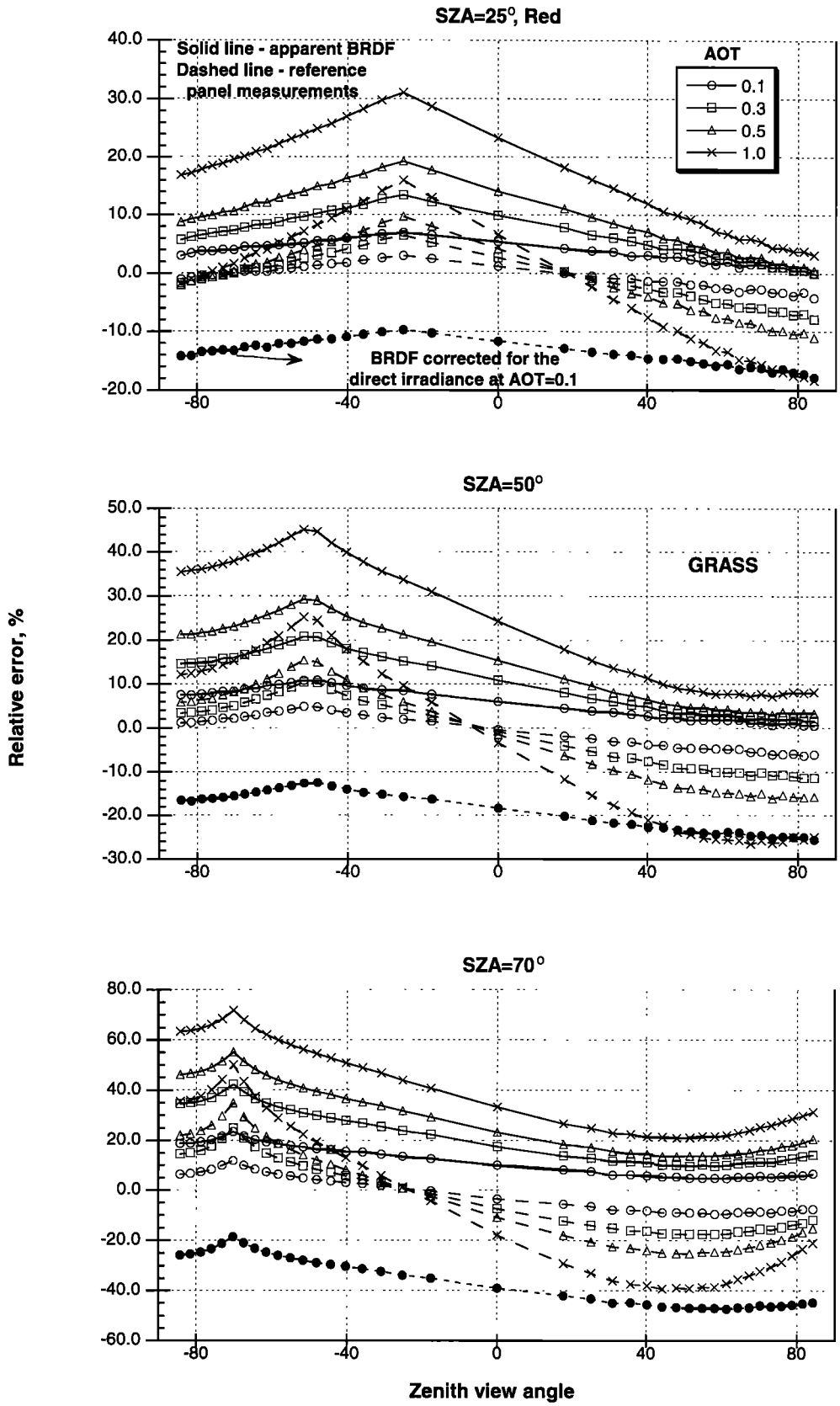

Figure 5a. Relative errors of typical experimental BRDF characterization in the principal plane for grass in the visible part of spectrum. AOT is aerosol optical thickness.

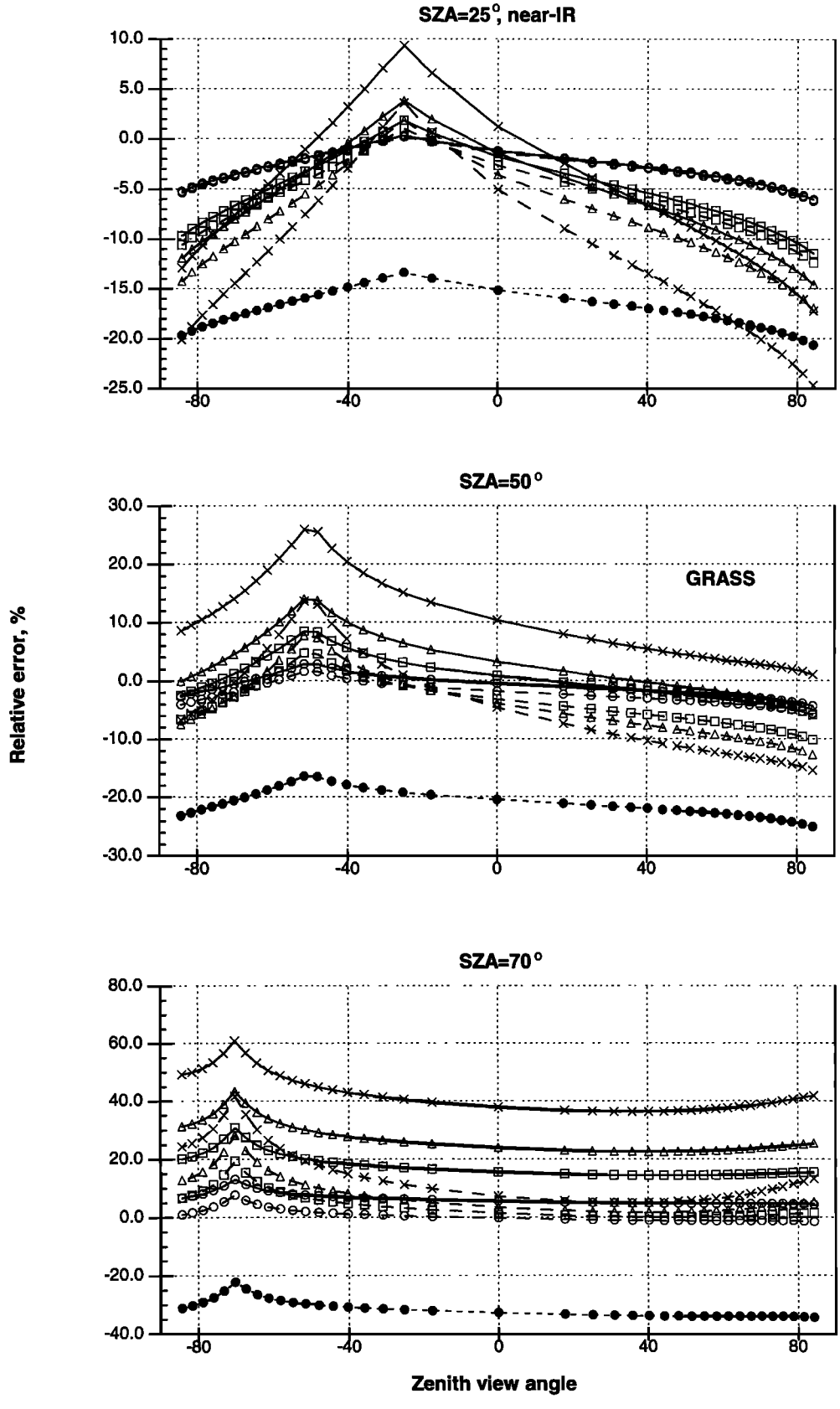

Figure 5b. The same as Figure 5a, but for near-IR.

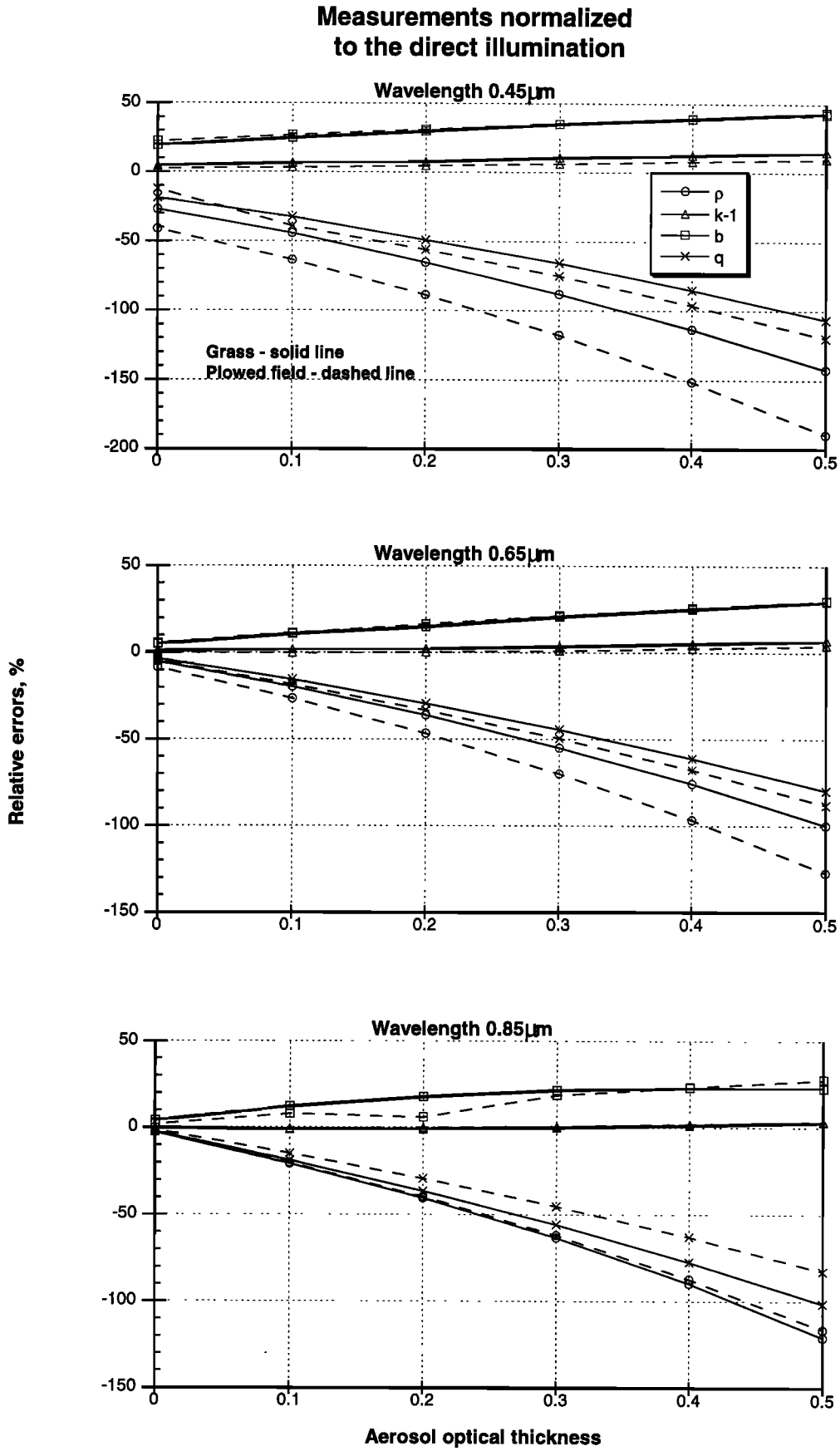

Figure 6a. Relative errors in parameters of the modified Rahman-Pinty-Verstraete BRDF model [*Martonchik et al.*, 1998] and in surface albedo for measurements normalized to the direct solar illumination.

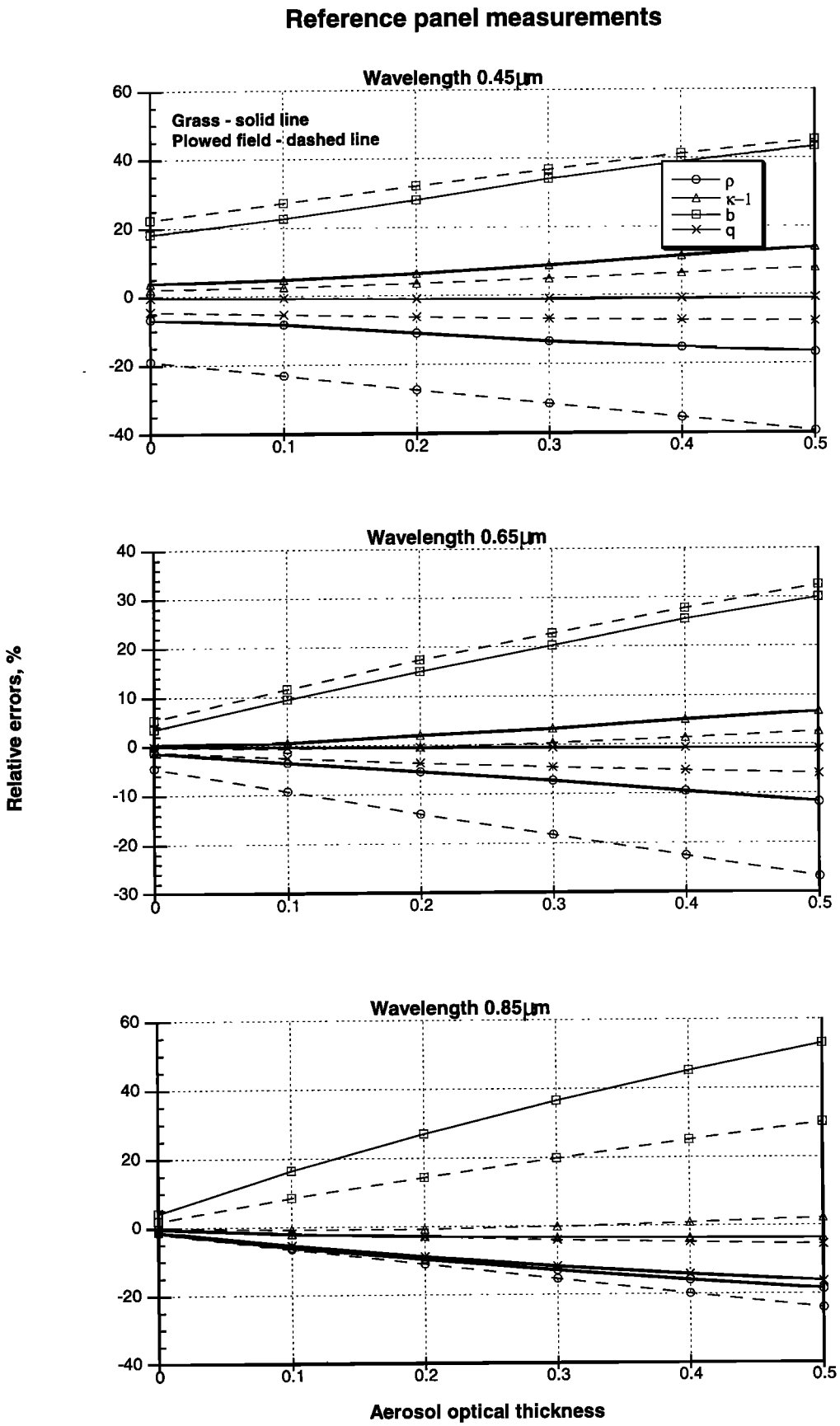

Figure 6b. The same as Figure 6a, but for measurements normalized to the total illumination.

this point, however, we cannot make a good judgement about the sufficiency of this accuracy. The answer to this question should come from practical applications such as land cover classification or the derivation of physical surface properties.

One of the purposes of this work was to estimate errors in the uncorrected BRDF data usually reported in the literature. Our simulations have shown that the distortions of the BRDF shape are considerable even at low aerosol optical thickness. For example, the reference panel technique measures the BRDF with an error of up to ±12% in the red and ±8% in the near-IR at τ^a=0.1. These results suggest that the atmospheric correction should be a required step in the processing of field reflectance data.

Acknowledgments. This research was performed under USRA contract NAS5-32484 and EOS AM-1 validation funding. Some of the results were presented at the IGARSS'98. The authors are grateful to R. S. Fraser for his comments on the manuscript.

References

Deering, D. V., and P. Leone, A sphere-scanning radiometer for rapid directional measurements of sky and ground radiance, *Remote Sens. Environ.*, *19*, 1-24, 1986.

Deering, D. V., and T. F. Eck, Atmospheric optical depth effects on angular anisotropy of plant canopy reflectance, *Int. J. Remote Sens.*, *8*, 893-916, 1987.

DeHoop, A. T., Reciprocity theorem for the electromagnetic field scattered by an obstacle, *Appl. Sci. Res.*, *8, ser. B*, 135-140, 1960.

Eaton, F. D., and I. Dirmhirn, Reflected irradiance indicatrices of natural surfaces and their effect on albedo, *Appl. Opt.*, *18*(7), 994-1008, 1979.

Elterman, L., UV, visible and IR attenuation for altitudes to 50 km, *Environ. Res. Pap-s, AFCRL, NTIS-AD 671933*, 58 pp., Air Force Cambridge Res. Labs., Bedford, Mass., 1968.

Engelsen, O., B. Pinty, M. M. Verstraete, and J. V. Martonchik, Parametric bidirectional reflectance factor models: Evaluation, improvements and applications, *Eur. Rep. 16426 EN*, Space Appl. Inst., Ispra, Italy, 1996.

Henderson-Sellers, A., and M.F.Wilson, Surface albedo for climate modeling, *Rev. Geophys.*, *21*, 1743-1778, 1983.

Hobbs, P. V., J. S. Reid, R. A. Kotchenruther, R. J. Ferek, and R. Weiss, Direct radiative forcing by smoke from biomass burning, *Science*, *275*, 1776-1778, 1997.

Girolamo, L., T.Varnai, and R. Davies, Apparent breakdown of reciprocity in reflected solar radiances, *J. Geophys. Res.*, *103*, 8795-8803, 1998.

Kimes, D.S., and W.W. Newcomb, Directional scattering properties of a wintering decidious hardwood canopy, *IEEE Trans. Geosci. Remote Sens.*, *GE-25*, 510-515, 1987.

Kimes, D. S., W. W. Newcomb, R. F. Nelson, and J. B. Schutt, Directional reflectance distribution of a hardwood and pine forest canopy, *IEEE Trans. Geosci. Remote Sens.*, *GE-24*, 281-293, 1986.

Krekov G. M., and R. F. Rahimov, *The Model of Continental Aerosol Based on Optical Ranging of the Atmosphere* (in Russian), 197 pp., Novosibirsk, Russia, 1982.

Kriebel, K. T., The spectral reflectance of a vegetated surface (in German), *Contrib. Atmos. Phys.*, *47*, 14-44, 1974.

Kriebel, K. T., On the limited validity of reciprocity in measured BRDF's, *Remote Sens. Environ.*, *58*, 52-62, 1996.

Lee, T., and Y. J. Kaufman, The effect of surface non-Lambertianity on remote sensing of ground reflectance and vegetation index, *IEEE Trans. Geosci. Remote Sens.*, *GE-24*, 699-708, 1986.

Lyapustin, A. I., Atmospheric and geometrical effects on land surface albedo, *J. Geophys. Res.*, in press, 1999.

Lyapustin, A. I., and T. Z. Muldashev, Method of spherical harmonics in the radiative transfer problem with non-Lambertian surface, *J. Quant. Spectrosc. Radiat. Transfer*, *61* (4), 545-555, 1998.

Martonchik, J. V., Retrieval of surface directional reflectance properties using ground level multiangle measurements, *Remote Sens. Environ.*, *50*, 303-316, 1994.

Martonchik, J. V., D. J. Diner, B. Pinty, M. M. Verstraete, R. B. Myneni, Y. Knyazikhin, and H. R. Gordon, Determination of land and ocean reflective, radiative, and biophysical properties using multiangle imaging, *IEEE Trans. Geosci. Remote Sens.*, *36*, 1266-1281, 1998.

Mikhlin, S. G., *Integral equations*, in Pure and Applied Mathematics, vol. 4, edited by I. N. Sheldon, 338 pp., Pergamon, Tarrytown, N.Y., 1957.

Minnaert, M., The reciprocity principle in lunar photometry, *Astrophys. J.*, *1*, 403-410, 1941.

Myneni, R. B., and G. Asrar, Radiative transfer in three-dimensional atmosphere-vegetation media, *J. Quant. Spectrosc. Radiat. Transfer*, *49*, 585-598, 1993.

Press, W. H., S. A. Teukolsky, W. T. Vetterling, and B. F. Flannery, *Numerical recipes in FORTRAN*, 2nd ed., 963 pp., Cambridge Univ. Press, New York, 1992.

Privette, J. L., R. B. Myneni, C. J. Tucker, and W. J. Emery, Invertibility of a 1-D discrete ordinates canopy reflectance model, *Remote Sens. Environ.*, *48*, 89-105, 1994.

Privette, J. L., T. F. Eck, and D. W. Deering, Estimating spectral albedo and nadir reflectance through inversion of simple BRDF models with AVHRR/MODIS-like data, *J. Geophys. Res.*, *102*, 29529-29542, 1997.

Rahman, H., B. Pinty, and M. M. Verstraete, Coupled surface-atmosphere reflectance (CSAR) model. 2. Semiempirical surface model usable with NOAA advanced very high resolution radiometer data, *J. Geophys. Res.*, *98*, 20,791-20,801, 1993.

Sellers, P. J., Remote sensing of the land surface for studies of global change, *NASA/GSFC Int. Satell. Land Surface Climatol.Proj. Rep.*, Columbia, Md., 1993.

Snyder, W. C., Reciprocity of the bidirectional reflectance distribution function (BRDF) in measurements and models of structured surfaces, *IEEE Trans. Geosci. Remote Sens.*, 36, 685-691, 1998.

Strahler, A. H., J. T. Townshend, D. Muchoney, J. Borak, M. Friedl, S. Gopal, A. Hyman, A. Moody, and E. Lambin, MODIS land cover and land cover change: Algorithm theoretical basis document, *NASA EOS MODIS Doc.*, ver. 4.1, 102 pp., 1996.

Vermote, E. F., N. El Saleos, C. O. Justice, Y. J. Kaufman, J. L. Privette, L. Remer, J. C. Roger, and D. Tanre, Atmospheric correction of visible to middle-infrared EOS- MODIS data over land surfaces: Background, operational algorithm and validation, *J. Geophys. Res.*, *102*, 17,131-17,141, 1997.

A. I. Lyapustin, Universities Space Research Association, NASA Goddard Space Flight Center, Mail Code 920, Greenbelt, MD 20771. (alyapust@pop900. gsfc.nasa.gov)

J. L. Privette, NASA Goddard Space Flight Center, Mail Code 923, Greenbelt, MD 20771.

(Received August 16, 1998; revised December 7, 1998; accepted December 17, 1998.)